Journal of Marine Science and Technology

Volume 25 | Issue 4 Article 3

OBLIQUE WAVE SCATTERING BY A SUBMERGED POROUS BREAKWATER WITH A PARTIALLY REFLECTING SIDEWALL

Yang Zhao
Shandong Provincial Key Laboratory of Ocean Engineering, Ocean University of China, Qingdao, China.

Hua-jun Li
Shandong Provincial Key Laboratory of Ocean Engineering, Ocean University of China, Qingdao, China.,
huajun@ouc.edu.cn

Yong Liu
Shandong Provincial Key Laboratory of Ocean Engineering, Ocean University of China, Qingdao, China.

OBLIQUE WAVE SCATTERING BY A SUBMERGED POROUS BREAKWATER WITH A PARTIALLY REFLECTING SIDEWALL

Acknowledgements

This study was supported by the Natural Science Foundation of China under Grant numbers 51490675, 51322903 and 51279224.

Journal of Marine Science and Technology, Vol. 25, No. 4, pp. 383-392 (2017)
DOI: 10.6119/JMST-017-0306-1

OBLIQUE WAVE SCATTERING BY A SUBMERGED POROUS BREAKWATER WITH A PARTIALLY REFLECTING SIDEWALL

Yang Zhao, Hua-jun Li, and Yong Liu

Key words: submerged porous breakwater, partially reflecting sidewall, oblique wave, analytical solution.

ABSTRACT

This study develops an analytical solution for oblique wave scattering by a submerged porous breakwater with a leeside partially reflecting vertical wall. The matched eigenfunction expansion method is used to develop the analytical solution. The whole fluid domain is divided into three regions according to the geometries of the structures. The series solution of the velocity potential in each region is obtained by the separation of the variables, and the unknown expansion coefficients are determined using the pressure and velocity continuous conditions on interfaces of different regions. The newly developed analytical solution is confirmed by an independently developed multi-domain boundary element method (BEM) solution and two known solutions for special cases. Numerical examples are presented to examine the reflection and transmission coefficients of the porous breakwater. Some useful results for engineering design are provided. The present solution may be used to determine the optimal breakwater parameters under an oblique wave attack at a preliminary engineering design stage.

I. INTRODUCTION

Submerged porous breakwaters can provide environmentally friendly protection for coast lines and coastal structures and, thus, are often used in coastal engineering. For example, offshore submerged porous breakwaters have been successfully used to protect the Gudong Sea Dike and the Zhuangxi Sea Dike in the Shengli Oil Field in China (Liao et al., 2006). The water wave interactions with the submerged porous breakwaters have been well studied by many researchers using analytical, numerical and experimental methods (Yu and Chwang, 1994; Losada et al., 1996; Twu and Liu, 2004; Lara et al., 2006; Cheng et al., 2009; Lan et al., 2011; Zhang et al., 2012; Liao et al., 2013; Lee et al., 2014; Wu et al., 2014; among others). These studies have provided scientific insights regarding the problems. In these studies, the hydrodynamic performance of submerged porous breakwaters was examined alone, and the effects of leeside structures were not considered.

When a submerged porous breakwater is used to protect a seawall or steep coastal cliff, the hydrodynamic performance of the porous breakwater can be significantly changed by the reflection off a seawall or cliff. Such effects should be considered in engineering design. Jeng et al. (2005) experimentally examined wave interactions among a submerged porous breakwater, a leeside vertical wall and a porous sand bed. They found that the strong interaction of the water waves between the porous breakwater and the vertical wall significantly changed the pore water pressure within the sand bed. Muni-Reddy and Neelamani (2006) experimentally measured the wave force reduction on a caisson protected by a submerged porous breakwater. By solving modified time-dependent mild-slope equations, Tsai et al. (2012) calculated the wave height transformation and setup between a submerged porous breakwater and a seawall. They clearly observed the modulations of the wave profile and wave setup between the breakwater and the seawall. Koraim et al. (2014) experimentally examined the reflection coefficient and the wave run-up on a vertical porous seawall with and without a seaside submerged breakwater. Recently, Koley et al. (2015) developed an analytical solution for wave trapping between a submerged porous bar and a fully reflecting vertical wall. They found that through a suitable design, a major part of the incident wave energy could be dissipated by the porous breakwater. Ko et al. (2015) numerically simulated wave and flow variations between dual submerged porous breakwaters and a slope seawall. They observed periodic spatial variations of the wave height and water level due to the wave reflection by the seawall and the submerged porous breakwaters.

In practice, a seawall or steep cliff is generally a partially reflecting structure (Goda, 2010, Table 3.8; Elchahal et al., 2008), which should be rather different from a fully reflecting structure. This study will develop a new analytical solution for oblique wave scattering by a submerged porous breakwater with a leeside

Paper submitted 04/25/16; revised 08/24/16; accepted 03/06/17. Author for correspondence: Hua-jun Li (e-mail: huajun@ouc.edu.cn).
Shandong Provincial Key Laboratory of Ocean Engineering, Ocean University of China, Qingdao, China.

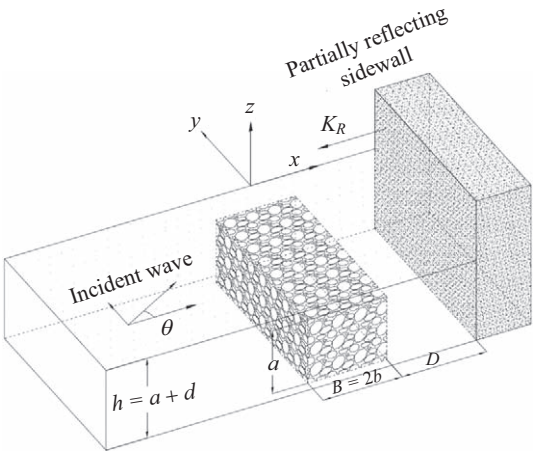

Fig. 1. Sketch of oblique wave scattering by a submerged porous breakwater with a partially reflecting sidewall.

partially reflecting wall and present useful results for engineering applications. In the following section, the boundary value problem for oblique wave scattering by a submerged porous breakwater with a partially reflecting sidewall is formulated. The partially reflecting boundary condition proposed by Isaacson and Qu (1990) is used to represent the effect of the sidewall. The wave energy dissipation by the porous breakwater is described using the classical porous medium model proposed by Sollitt and Cross (1972). In section 3, the analytical solution for the present problem is developed using the matched eigenfunction expansion method. In section 4, the analytical solution is validated by previous solutions for special cases and an independently developed multi-domain BEM solution for the present problem. Numerical examples are presented to examine the reflection and transmission coefficients of the porous breakwater. Finally, the main conclusions of this study are drawn.

II. MATHEMATICAL FORMULATION

The idealized sketch of oblique wave scattering by a submerged porous breakwater with a leeside partially reflecting sidewall is shown in Fig. 1. A Cartesian coordinate system, with an x-y plane located on the still water level and the z-axis directing upwards along the vertical midline of the porous breakwater, is adopted. The water depth is h, and the wave approaches the breakwater at an angle θ ($0° \le \theta < 90°$) to the positive x-axis. The incident wave number k_0 has the components of $k_{0x} = k_0 \cos\theta$ and $k_{0y} = k_0 \sin\theta$ in the x- and y-directions, respectively. It is noted that the special case of a normal incident wave with $\theta = 0°$ can be directly analysed by the present solution. However, the limiting case of $\theta = 90°$ cannot be considered by the present solution. The width and the height of the porous breakwater are B ($B = 2b$) and a, respectively. The submerged depth of the porous breakwater is d ($d = h - a$). The spacing between the porous breakwater's rear face and the partially reflecting side wall is D. The reflection coefficient of the sidewall is K_R. The lengths of the porous breakwater and the sidewall along the y-direction are assumed to be infinite as they are very large compared to the incident wavelength. For the solution of the problem, the whole fluid domain is divided into the following three regions: region 1 is the fluid domain in front of the porous breakwater ($x \le -b$, $-h \le z \le 0$); region 2 includes the fluid domains above and inside the porous breakwater ($-b \le x \le b$, $-h \le z \le 0$); and region 3 is the fluid domain between the porous breakwater and the sidewall ($b \le x \le b + D$, $-h \le z \le 0$).

The present analytical solution is developed based on the linear potential theory and the classical porous medium model proposed by Sollitt and Cross (1972). The fluid motions inside and outside the porous breakwater are both described by a velocity potential $\Phi(x, y, z, t)$. For time-harmonic incident waves with angular frequency ω, the velocity potential is further written as:

$$\Phi(x, y, z, t) = \mathrm{Re}\left\{-\frac{igH}{2\omega}\phi(x, z)\mathrm{e}^{\mathrm{i}k_{0y}y}\,\mathrm{e}^{-\mathrm{i}\omega t}\right\}, \tag{1}$$

where Re denotes the real part of the variables, g is the gravitational acceleration, H is the incident wave height, and $\phi(x, z)$ is a complex spatial velocity potential.

The spatial velocity potential in each region satisfies the modified Helmholtz equation:

$$\frac{\partial^2\phi_j}{\partial x^2} + \frac{\partial^2\phi_j}{\partial z^2} - k_{0y}^2\phi_j = 0\,,\ j = 1, 2, 3\,, \tag{2}$$

where the subscript j denotes the variables in region j. The velocity potentials also satisfy the following boundary conditions:

$$\frac{\partial\phi_j}{\partial z} = \frac{\omega^2}{g}\phi_j\,,\ z = 0\,,\ j = 1, 2, 3\,, \tag{3}$$

$$\frac{\partial\phi_j}{\partial z} = 0\,,\ z = -h\,,\ j = 1, 2, 3\,, \tag{4}$$

$$\left.\frac{\partial\phi_2}{\partial z}\right|_{z=-d^+} = \varepsilon\left.\frac{\partial\phi_2}{\partial z}\right|_{z=-d^-}, \tag{5}$$

$$\left.\phi_2\right|_{z=-d^+} = (s + \mathrm{i}f)\left.\phi_2\right|_{z=-d^-}, \tag{6}$$

where $z = -d^+$ and $z = -d^-$ denotes, respectively, the upper and lower sides of the porous breakwater horizontal surface, and ε, f and s are, respectively, the porosity, the linearized resistance coefficient and the inertial coefficient of the porous breakwater (Sollitt and Cross, 1972; Dalrymple et al., 1991; Yu and Chwang, 1994). Here, the effect of the porous breakwater (porous medium) is represented by the three parameters of ε, f and s. When $\varepsilon = 1$, $f = 0$ and $s = 1$, the porous medium becomes water. In addition to the preceding boundary conditions, the reflected wave in region 1 propagates along the specular reflection direction of the incident wave and must be outgoing in the far field.

The preceding Eqs. (2)-(6) formulate a complete boundary value problem for oblique wave scattering by a submerged porous breakwater with a partially reflecting sidewall.

III. ANALYTICAL SOLUTIONS

The series solutions of the velocity potentials, which satisfy Eq. (2) and the relevant boundary conditions in Eqs. (3)-(6), can be written as:

$$\phi_1 = \mathrm{e}^{\mathrm{i}k_{0x}(x+b)} Z_0(z) + R_0 \mathrm{e}^{-\mathrm{i}k_{0x}(x+b)} Z_0(z) + \sum_{m=1}^{\infty} R_m \mathrm{e}^{k_{mx}(x+b)} Z_m(z), \tag{7}$$

$$\phi_2 = \sum_{m=0}^{\infty} \left(A_m \cos \lambda_{mx} x + B_m \sin \lambda_{mx} x \right) Y_m(z), \tag{8}$$

$$\phi_3 = C_0 \mathrm{e}^{\mathrm{i}k_{0x}(x-b)} Z_0(z) + D_0 \mathrm{e}^{-\mathrm{i}k_{0x}(x-b-D)} Z_0(z) + \sum_{m=1}^{\infty} \left[C_m \mathrm{e}^{-k_{mx}(x-b)} + D_m \mathrm{e}^{k_{mx}(x-b-D)} \right] Z_m(z), \tag{9}$$

where R_m, A_m, B_m, C_m and D_m are unknown expansion coefficients, and $Z_m(z)$ and $Y_m(z)$ are vertical eigenfunctions given by (Losada et al., 1996):

$$Z_0(z) = \frac{\cosh k_0 (z+h)}{\cosh k_0 h}, \tag{10a}$$

$$Z_m(z) = \frac{\cos k_m (z+h)}{\cos k_m h}, \ m \geq 1, \tag{10b}$$

$$Y_m(z) = \frac{\cosh \lambda_m (z+h) - P_m \sinh \lambda_m (z+h)}{\cosh \lambda_m h - P_m \sinh \lambda_m h}, \quad -d \leq z \leq 0, \quad m \geq 0, \tag{11a}$$

$$Y_m(z) = \frac{1 - P_m \tanh \lambda_m a}{s + \mathrm{i}f} \frac{\cosh \lambda_m (z+h)}{\cosh \lambda_m h - P_m \sinh \lambda_m h}, \quad -h \leq z < -d, \quad m \geq 0, \tag{11b}$$

$$P_m = \frac{\left[1 - \varepsilon / (s + \mathrm{i}f) \right] \tanh \lambda_m a}{1 - \varepsilon / (s + \mathrm{i}f) \tanh^2 \lambda_m a}, \ m \geq 0, \tag{12}$$

in which $k_{mx} = \sqrt{k_{0y}^2 + k_m^2}$ ($m \geq 1$), $\lambda_{mx} = \sqrt{\lambda_m^2 - k_{0y}^2}$ (m ≥ 0),

Table 1. Calculation results for the complex wave numbers at $k_0 d = 1.5$, $a/h = 0.5$, $\varepsilon = 0.4$, $f = 2.0$ and $s = 1.0$.

Complex wave numbers	Calculation results
λ_0	2.416523 + 0.328700 i
λ_1	0.122608 + 2.161902 i
λ_2	0.032153 + 5.955472 i
λ_3	0.110965 – 9.783322 i
λ_4	0.410217 –13.372354 i

and the positive real numbers k_m and the complex wave numbers λ_m satisfy:

$$\omega^2 = g k_0 \tanh k_0 h = -g k_m \tan k_m h, \ m \geq 1, \tag{13}$$

$$\omega^2 - g \lambda_m \tanh \lambda_m h = P_m \left(\omega^2 \tan \lambda_m h - g \lambda_m \right), \ m \geq 0. \tag{14}$$

In this study, the wave numbers above and inside the submerged porous breakwater in region 2 are assumed to be the same. Then, the vertical eigenfunctions in Eq. (11) and the complex dispersion relationship in Eq. (14) are developed using the free surface condition, Eq. (3), the water bottom condition, Eq. (4), and the vertical velocity and pressure continuous conditions on the upper horizontal surface of the submerged porous breakwater, Eqs. (5) and (6). More details can be found in Losada et al. (1996) and Neves et al. (2000).

We use the Newton-Raphson method to find the complex roots of Eq. (14). In our calculations, the initial guesses of all the complex roots are determined using the perturbation method proposed by Mendez and Losada (2004). The initial guesses of the complex roots can also be obtained by the homotopy perturbation method proposed by Chang and Liou (2006). The typical calculation results of the complex wave numbers are listed in Table 1. The real and imaginary parts of a complex wave number denote the spatial scale of the wavelength and the damping modulus of the wave amplitude above the submerged porous breakwater, respectively.

On the interfaces between adjacent regions ($x = \pm b$), the velocity potential and the horizontal mass fluxes must be continuous:

$$\phi_1 = \alpha \phi_2, \ x = -b, \tag{15}$$

$$\frac{\partial \phi_1}{\partial x} = \beta \frac{\partial \phi_2}{\partial x}, \ x = -b, \tag{16}$$

$$\phi_3 = \alpha \phi_2, \ x = b, \tag{17}$$

$$\frac{\partial \phi_3}{\partial x} = \beta \frac{\partial \phi_2}{\partial x}, \ x = b, \tag{18}$$

where $\alpha = \beta = 1$ ($-d \leq z \leq 0$), $\alpha = s + if$ ($-h < z < -d$) and $\beta = \varepsilon$ ($-h < z < -d$).

On the leeside vertical wall, the partially reflecting boundary condition for obliquely incident waves is given by (Isaacson and Qu, 1990):

$$\frac{\partial \phi_3}{\partial x} = \mu k_{0x} \phi_3 \,,\ \mu = \mathrm{i}\frac{1-K_R}{1+K_R} \,,\ x = b + D \,, \tag{19}$$

where K_R is the reflection coefficient of the sidewall as mentioned in Fig. 1. When using Eq. (19), the wave incident direction in front of the sidewall is the same as that from the open sea. In addition, the reflection phase angle on the sidewall is simply treated as zero according to the numerical results presented by Isaacson and Qu (1990). When K_R is equal to unity, the transmitted waves by the porous breakwater are fully reflected by the sidewall. While K_R is equal to zero, the transmitted propagation waves are fully dissipated by the sidewall. In practice, the reflection coefficient K_R of a seawall should be determined by experimental tests or field tests. Alternatively, the approximate reflection coefficients of typical coastal structures can be found in Goda (2010, Table 3.8).

We note that the partially reflecting boundary condition in Eq. (19) in fact denotes the wave energy dissipation by the wave absorber behind the boundary. This is very different from the porous boundary condition presented by Yu (1995), which denoted the pressure loss on a perforated thin wall, i.e., the wave energy dissipation by the porous boundary itself.

Next, we can use the boundary conditions in Eqs. (15)-(19) to determine the unknown expansion coefficients in the velocity potentials. Upon inserting the velocity potentials from Eqs. (7) and (8) into Eq. (15), we have:

$$\begin{aligned} & Z_0(z) + \sum_{m=0}^{\infty} R_m Z_m(z) \\ & = \sum_{m=0}^{\infty} \alpha \left(A_m \cos \lambda_{mx} b - B_m \sin \lambda_{mx} b \right) Y_m(z), \\ & -h \le z \le 0. \end{aligned} \tag{20}$$

Multiplying both sides of Eq. (20) by $Z_n(z)$ and integrating with respect to z along the whole water depth, we have:

$$\delta_{0n} + R_n = \sum_{m=0}^{\infty} \frac{\Lambda_{mn}}{\Gamma_n} \left(A_m \cos \lambda_{mx} b - B_m \sin \lambda_{mx} b \right) ,\ n \ge 0 \,, \tag{21}$$

where $\delta_{mn} = 1$ $(m = n)$, $\delta_{mn} = 0$ $(m \ne n)$, $\Lambda_{mn} = \int_{-h}^{0} \alpha Y_m(z) Z_n(z) \mathrm{d}z$, and $\Gamma_n = \int_{-h}^{0} Z_n^2(z) \mathrm{d}z$. Using a similar method as Eq. (21), we transform Eqs. (16)-(19) into

$$-\delta_{0n} + R_n = \sum_{m=0}^{\infty} \frac{\lambda_{mx} \Omega_{mn}}{\tilde{k}_{nx} \Gamma_n} \left(A_m \sin \lambda_{mx} b + B_m \cos \lambda_{mx} b \right), n \ge 0, \tag{22}$$

$$C_n + \mathrm{e}^{-\tilde{k}_{nx} D} D_n = \sum_{m=0}^{\infty} \frac{\Lambda_{mn}}{\Gamma_n} \left(A_m \cos \lambda_{mx} b + B_m \sin \lambda_{mx} b \right), n \ge 0, \tag{23}$$

$$-C_n + \mathrm{e}^{-\tilde{k}_{nx} D} D_n = \sum_{m=0}^{\infty} \frac{\lambda_{mx} \Omega_{mn}}{\tilde{k}_{nx} \Gamma_n} \left(-A_m \sin \lambda_{mx} b + B_m \cos \lambda_{mx} b \right), n \ge 0, \tag{24}$$

$$\left(\mu k_{0x} + \tilde{k}_{nx} \right) \mathrm{e}^{-\tilde{k}_{nx} D} C_n + \left(\mu k_{0x} - \tilde{k}_{nx} \right) D_n = 0 \,,\ n \ge 0 \,, \tag{25}$$

where $\tilde{k}_{0x} = -\mathrm{i} k_{0x}$, $\tilde{k}_{nx} = k_{nx}$ ($n \ge 1$) and $\Omega_{mn} = \int_{-h}^{0} \beta Y_m(z) Z_n(z) \mathrm{d}z$.

We truncate n and m after N terms in Eqs. (21)-(25) and solve the equations simultaneously using the standard Gauss elimination method to determine the velocity potentials.

The reflection and transmission coefficients of a coastal structure are defined as the ratios of the reflected and transmitted propagation wave heights to the incident wave height, respectively. In Eq. (7), the first term is the incident waves, the second term is the reflected propagation waves in front of the submerged breakwater, and the third term represents a series of evanescent modes decaying in the negative x-direction. In Eq. (9), the first term represents the transmitted propagation waves, and the second term is the propagation waves reflected by the sidewall. Thus, the reflection coefficient C_R and the transmission coefficient C_T of the porous breakwater are:

$$C_R = \left| R_0 \right| , \tag{26}$$

$$C_T = \left| C_0 \right| . \tag{27}$$

We conclude in theory that the reflection coefficient of the partially reflecting sidewall satisfies:

$$K_R = \left| \frac{D_0}{C_0} \right| . \tag{28}$$

This relationship can be used to assess the accuracy of our present analytical results. By considering the wave energy conservation, the energy loss coefficient of the submerged porous breakwater can be defined as:

$$E_L = 1 - C_R^2 - C_T^2 + \left(K_R C_T \right)^2 . \tag{29}$$

IV. RESULTS WITH DISCUSSIONS

1. Convergence Examination

We first examine the convergence of the present series solution by increasing the truncated number N adopted for solving Eqs. (21)-(25). The calculated reflection and transmission coefficients, C_R and C_T, at different N values for a typical case are listed in Table 2. The calculation conditions are as follows: $k_0 d = 1.5$, $a/h = 0.8$, $B/h = 0.8$, $D/h = 3.0$, $\varepsilon = 0.4$, $f = 2.0$, $s = 1.0$ and $K_R = 0.5$. It can be observed from Table 2 that the value of $N = 40$ should be enough to obtain convergent results. Thus, the value of $N = 40$ is adopted in this study.

Table 2. Convergence of C_R and C_T with the increasing truncated number N.

N	$\theta = 10°$		$\theta = 30°$		$\theta = 50°$		$\theta = 80°$	
	C_R	C_T	C_R	C_T	C_R	C_T	C_R	C_T
2	0.4270	0.6233	0.4045	0.6699	0.4194	0.6276	0.7678	0.3416
5	0.3810	0.5898	0.3962	0.6473	0.3831	0.5996	0.7520	0.3374
10	0.3830	0.5921	0.3956	0.6482	0.3850	0.6018	0.7518	0.3381
20	0.3832	0.5926	0.3955	0.6484	0.3854	0.6021	0.7517	0.3382
40	0.3832	0.5927	0.3954	0.6484	0.3854	0.6022	0.7517	0.3382
60	0.3832	0.5927	0.3954	0.6484	0.3855	0.6022	0.7517	0.3382

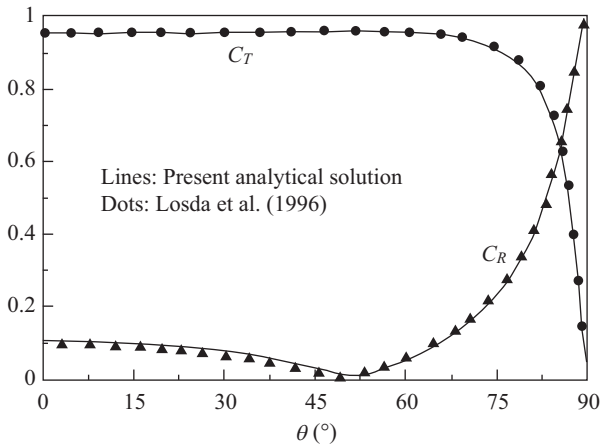

Fig. 2. Comparison between the present analytical solution and that presented by Losada et al. (1996).

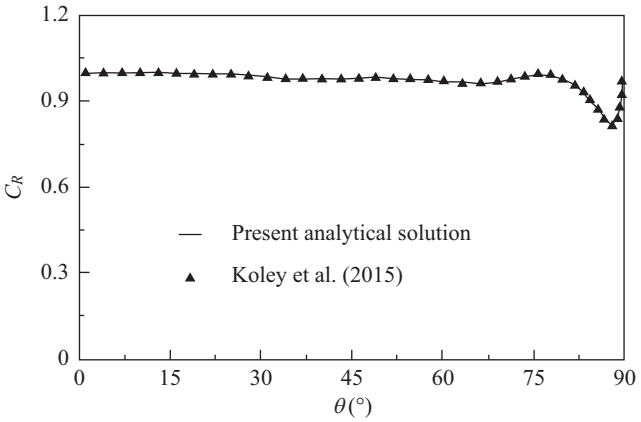

Fig. 3. Comparison between the present analytical solution and that presented by Koley et al. (2015).

2. Comparison with Known Solutions of Special Cases

Losada et al. (1996) developed an analytical solution for oblique wave scattering by a submerged porous breakwater without a leeside vertical wall. When the reflection coefficient K_R of the present sidewall is zero and the distance D between the porous breakwater and the sidewall is large enough, the present solution becomes the analytical solution presented by Losada et al. (1996). The reflection and transmission coefficients calculated by the present analytical solution are compared with the results presented by Losada et al. (1996), as shown in Fig. 2. The calculation conditions are as follows: $k_0h = 0.68$, $a/h = 0.7$, $B/h = 1.0$, $D/h = 10.0$, $\varepsilon = 0.4$, $f = 1.5$, $s = 1.0$ and $K_R = 0$. It can be observed from Fig. 2 that the two solutions are in good agreement. Additionally, it can be observed from this figure that with the increasing wave incident angle θ, the reflection coefficient first decreases, attains its minimum and then rapidly increases to unity.

Koley et al. (2015) developed an analytical solution for oblique wave scattering by a submerged porous breakwater in front of a fully reflecting vertical sidewall. When the reflection coefficient of the present sidewall is unity, the present solution becomes the analytical solution presented by Koley et al. (2015). The reflection coefficients C_R calculated by the present analytical solution are compared with the results presented by Koley et al. (2015), as shown in Fig. 3. The calculation conditions are as follows: $k_0h = 0.592$, $a/h = 0.2$, $B/h = 0.6$, $D/h = 10.607$, $\varepsilon = 0.437$, $f = 0.5$, $s = 1.0$ and $K_R = 1.0$. Again, the two solutions are in good agreement.

3. Comparison with Multi-Domain BEM Solution

In addition to the analytical solution, we develop a multi-domain boundary element method (BEM) solution for the present oblique wave scattering problem. The present multi-domain BEM solution is given in the Appendix, which is modified by our previous BEM solution for normally incident waves (Liu et al., 2012). The multi-domain BEM solution is a numerical solution, and it needs the discretizing of all the boundaries of fluid domains. Thus, the solution procedure of the BEM solution is more cumbersome than the analytical solution, but the BEM solution can consider structures with more complicated shapes. More details on the multi-domain BEM can be found in Ijima et al. (1976), Sulisz (1985), Yueh and Chuang (2009) and others.

The reflection coefficients C_R calculated by the analytical solution and the multi-domain BEM solution are compared in Fig. 4 for cross-checking. The calculation conditions are as follows: $a/h = 0.5$, $B/h = 1.0$, $D/h = 1.0$, $\varepsilon = 0.45$, $f = 2.0$, $s = 1.0$

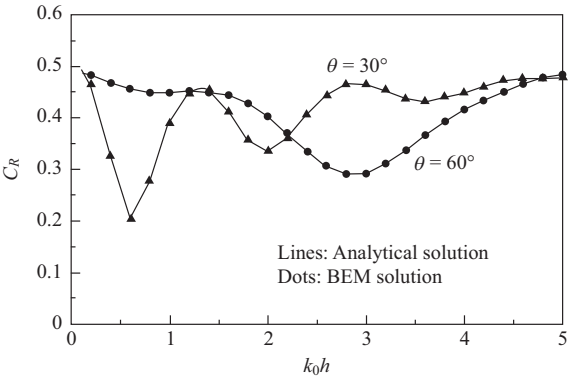

Fig. 4. Comparison between the present analytical solution and the multi-domain BEM solution.

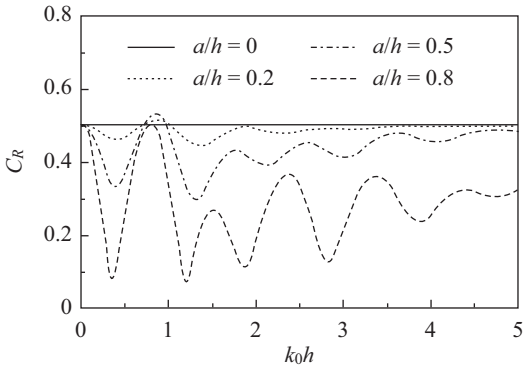

(a) The reflection coefficient C_R

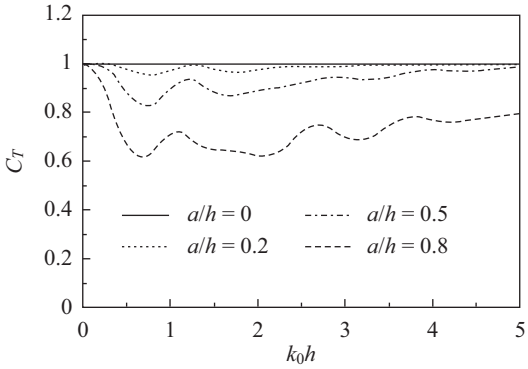

(b) The transmission coefficient C_T

Fig. 5. Effects of the relative breakwater height *a*/*h* on the reflection and transmission coefficients.

and $K_R = 0.5$. It can be observed from Fig. 4 that the agreement between the two solutions is very good.

According to the preceding validations, we believe that the solving procedure of the present analytical solution should be correct.

4. Numerical Examples

We first present Fig. 5 to examine the effects of the relative porous breakwater height a/h on the reflection coefficient C_R and the transmission coefficient C_T. The calculation conditions are as follows: $\theta = 30°$, $B/h = 0.8$, $D/h = 3.0$, $\varepsilon = 0.4$, $f = 2.0$, $s = 1.0$ and $K_R = 0.5$. It can be observed from Fig. 5 that the reflection and transmission coefficients both decrease with the increasing breakwater height. One may feel intuitively that when the breakwater height increases, the reflection coefficient should also increase. However, a higher submerged porous breakwater with a sidewall can dissipate more incident wave energy and, thus, results in a lower reflection coefficient. Our further calculation results show that when the porosity ε is small, the reflection coefficient C_R may increase with the increasing relative breakwater height a/h. In addition, the reflection coefficient of a submerged porous breakwater without a sidewall generally increases with the increasing value of a/h. We also note from Fig. 5(a) that with the increasing value of k_0h, the reflection coefficient oscillates between its local maximum and minimum values. This is due to the wave resonance between the porous breakwater and the sidewall.

The effects of the sidewall reflection coefficient K_R and the relative porous breakwater width B/h on the hydrodynamic quantities are shown in Figs. 6 and 7, respectively. As shown in these figures, the hydrodynamic quantities are plotted as the function of the relative spacing between the porous breakwater and the sidewall (the ratio of the spacing D to the incident wavelength L). The calculation conditions in Fig. 6 are as follows: $\theta = 30°$, $k_0h = 1.5$, $a/h = 0.8$, $B/h = 0.8$, $\varepsilon = 0.4$, $f = 2.0$ and $s = 1.0$. We note from Fig. 6 that for $K_R = 0$, the reflection and transmission coefficients are both constant, except for when the values of D/L are very small. This is because of the evanescent modes in Eq. (9) at small values of D/L. When the sidewall reflection coefficient K_R increases, the reflection and transmission coefficients both vary periodically with the increasing values of D/L. In addition, the reflection coefficient increases significantly with the increasing values of K_R, and the minimum transmission coefficient decreases with the increasing K_R. The calculation conditions in Fig. 7 are as follows: $\theta = 30°$, $k_0h = 1.5$, $a/h = 0.8$, $\varepsilon = 0.4$, $f = 2.0$, $s = 1.0$ and $K_R = 0.5$. It can be observed from Fig. 7 that a wider porous breakwater has a better sheltering function (with a lower transmission coefficient). However, the effect of the relative porous breakwater width on the reflection coefficient is rather complicated due to the interfaces of the waves reflected by the porous breakwater and the sidewall. By considering both Figs. 6 and 7, the relative spacing of D/L has significant effects on the hydrodynamic quantities of the porous breakwater in front of a partially reflecting sidewall. In practical engineering design, one should carefully design the value of D/L to obtain a lower transmission coefficient.

It should be mentioned that when the value of D/L approaches zero, the submerged porous breakwater is attached to the sidewall. For this special case, the transmission coefficient C_T defined in Eq. (27) is not zero and has little physical meaning. In fact, the wave reflection by a submerged porous bar attached to a fully reflecting vertical wall has been studied by Chen et al. (2006).

In the preceding numerical examples, the wave incident angle is fixed at $\theta = 30°$. As shown in Fig. 8, the reflection and transmis-

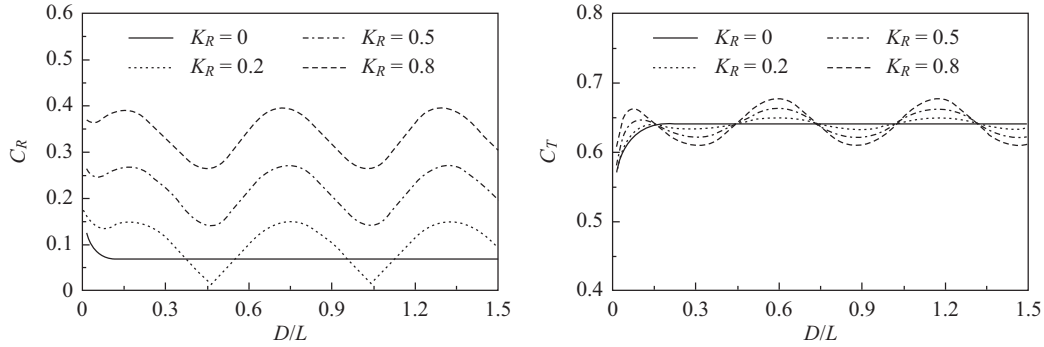

(a) The reflection coefficient C_R (b) The transmission coefficient C_T

Fig. 6. Effects of the sidewall reflection coefficient K_R on the reflection and transmission coefficients.

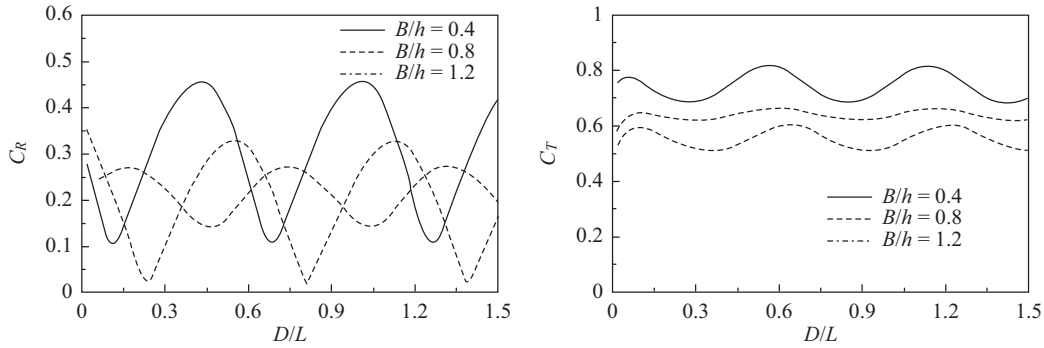

(a) The reflection coefficient C_R (b) The transmission coefficient C_T

Fig. 7. Effects of the relative breakwater width B/h on the reflection and transmission coefficients.

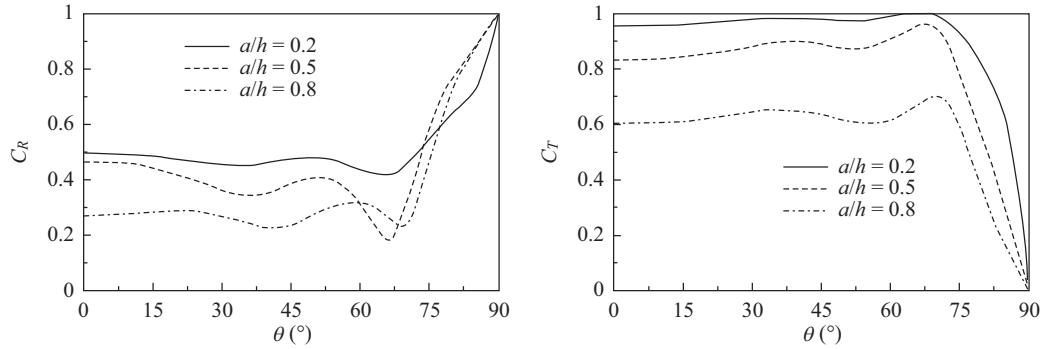

(a) The reflection coefficient C_R (b) The transmission coefficient C_T

Fig. 8. Effects of the wave incident angle θ on the reflection and transmission coefficients.

sion coefficients of the submerged porous breakwater at different wave incident angles are presented. The calculation conditions are as follows: $k_0h = 1.5$, $B/h = 0.8$, $D/h = 3.0$, $\varepsilon = 0.4$, $f = 2.0$, $s = 1.0$ and $K_R = 0.5$. When the wave incident angle increases from 0° to 60°, the variations of the reflection and transmission coefficients are not notable. While the wave incident angle further increases from 60° to 90°, the reflection coefficient and the transmission coefficient rapidly approach unity and zero, respectively. This is similar to the oblique wave reflection and transmission by a submerged porous breakwater without a sidewall, as shown in Fig. 2.

V. CONCLUDING REMARKS

We have used the matched eigenfunction expansion method to develop an analytical solution for oblique wave scattering by a submerged porous breakwater in front of a partially reflecting vertical wall. We have also developed a multi-domain BEM solution for the same problem. The hydrodynamic quantities of the reflection and transmission coefficients calculated by the analytical solution and the multi-domain BEM solution are in good

agreement. In addition, we have shown that for two special cases of a single submerged porous breakwater and a submerged porous breakwater with a fully reflecting sidewall, the present calculation results agree very well with previous results in the literature. The effects of major engineering design parameters, including the relative breakwater height and width, the sidewall reflection coefficient, and the relative spacing between the porous breakwater and the sidewall, on the reflection and transmission coefficients have been clarified by numerical examples. Due to wave resonance between the porous breakwater and the partially reflecting sidewall, the relative spacing between the porous breakwater and the sidewall must be carefully designed to obtain a lower transmission coefficient (better sheltering function). For preliminary engineering design, the present solution may be useful for determining the optimal breakwater parameters. It should be mentioned that the wave nonlinearity, the possible wave breaking over the submerged breakwater and the vortex flow near the structure cannot be considered in the present linear potential theory. These need to be clarified by further experimental tests and numerical simulations.

ACKNOWLEDGEMENTS

This study was supported by the Natural Science Foundation of China under Grant numbers 51490675, 51322903 and 51279224.

APPENDIX: MULTI-DOMAIN BEM SOLUTION

Here, the multi-domain boundary element method is used to solve the boundary value problem formulated in Section II. In the BEM solution, simple constant boundary elements are adopted. Fig. A.1 shows a sketch of the multi-domain BEM solution. The adopted Cartesian coordinate system is the same as that shown in Fig. 1. A fictional vertical boundary, which is far from the submerged porous breakwater, is set at $x = -l$ (beelines AB). Then, the whole fluid domain is divided into the following three regions: region 1 is the outer region ($x \le -l$); region 2 is the domain inside the porous breakwater and is enclosed by the curve DCFED; and region 3 is the fluid domain enclosed by the curve ABCDEFGHA.

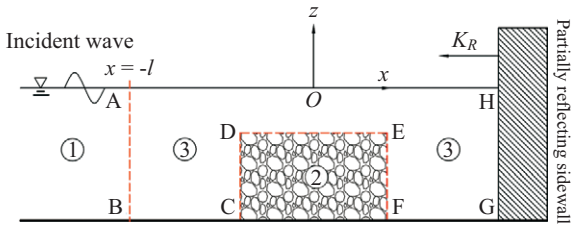

Fig. A.1. Sketch of the multi-domain BEM solution (side view).

The boundary integration equations for the velocity potentials in regions 2 and 3 can be written as (Ang, 2007):

$$\frac{1}{2}\phi_j(\xi,\eta)=\int_{\Gamma_j}\left[\phi_j(x,z)\frac{\partial G_j(x,z;\xi,\eta)}{\partial \boldsymbol{n}_j}-G_j(x,z;\xi,\eta)\frac{\partial \phi_j(x,z)}{\partial \boldsymbol{n}_j}\right]\mathrm{d}s(x,z),\ j=2,3, \tag{A.1}$$

where the subscript j denotes variables in region j; (ξ, η) and (x, z) denote, respectively, the source point and field point; Γ_j is the boundary curves of region j; $\boldsymbol{n}_j$ is the unit normal vectors on Γ_j and points away from region j; and the fundamental solution $G(x, z; \xi, \eta)$ of the modified Helmholtz equation is given by:

$$G(x,z;\xi,\eta)=-\frac{1}{2\pi}\mathrm{K}_0\left(k_{0y}\sqrt{(x-\xi)^2+(z-\eta)^2}\right), \tag{A.2}$$

in which K_0 is the modified Bessel function of the second kind of zero order.

All the boundary curves in regions 2 and 3 are divided into M_2 and M_3 beelines, respectively. On each beeline, the velocity potential and its normal derivative are constants. On the midpoint of the k-th boundary element of region j ($j = 2, 3$), the velocity potential and its normal derivative are written as $\varphi_{j,k}$ and $\overline{\varphi}_{j,k}$, respectively. Then, a discretized version of Eq. (A.1) is given by:

$$\left[\xi_{j,mk}\right]\left\{\varphi_{j,k}\right\}+\left[\zeta_{j,mk}\right]\left\{\overline{\varphi}_{j,k}\right\}=0\,,\ m,k=1,2,\ldots,M_j\,,j=2,3, \tag{A.3}$$

$$\xi_{j,mk}=\int_{\Gamma_{j,k}}\frac{\partial G_{j,k}\left(x,z;\xi,\eta\right)}{\partial \boldsymbol{n}_{j,k}}\mathrm{d}s\left(x,z\right)-\frac{1}{2}\delta_{mk}\,, \tag{A.4}$$

$$\zeta_{j,mk}=-\int_{\Gamma_{j,k}}G_{j,k}\left(x,z;\xi,\eta\right)\mathrm{d}s\left(x,z\right). \tag{A.5}$$

where, $\delta_{mk}=1$ ($m=k$), and $\delta_{mk}=0$ ($m\neq k$).

On the fictional boundary AB ($x=-l$), the velocity potentials and the horizontal fluid velocities are continuous:

$$\phi_1\left(-l,z\right)=\phi_3\left(-l,z\right), \tag{A.6}$$

$$\frac{\partial\phi_1}{\partial x}=\frac{\partial\phi_3}{\partial x}\,,\ x=-l\,. \tag{A.7}$$

The velocity potential in region 1 can be written as:

$$\phi_1=\left[\mathrm{e}^{\mathrm{i}k_{0x}\left(x+\ell\right)}+R_0\,\mathrm{e}^{-\mathrm{i}k_{0x}\left(x+\ell\right)}\right]Z_0\left(z\right), \tag{A.8}$$

where the evanescent modes are ignored as the outer region is far from the submerged porous breakwater. Inserting Eq. (A.8) into Eq. (A.6), then multiplying both sides of the new equation by $Z_0(z)$ and integrating with respect to z from $-h$ to 0 yields:

$$R_0=\frac{\int_{-h}^{0}\phi_3\left(-l,z\right)Z_0\left(z\right)\mathrm{d}z}{\int_{-h}^{0}Z_0^2(z)\,\mathrm{d}z}-1\,. \tag{A.9}$$

Substituting Eqs. (A.8) and (A.9) into Eq. (A.7), we have:

$$\frac{\partial\phi_3}{\partial x}=\mathrm{i}k_{0x}Z_0\left(z\right)\left[2-\frac{\int_{-h}^{0}\phi_3\left(-\ell,z\right)Z_0\left(z\right)\mathrm{d}z}{\int_{-h}^{0}Z_0^2(z)\,\mathrm{d}z}\right],\ \text{on AB.} \tag{A.10}$$

On the interface CDEF of regions 2 and 3, the velocity potentials satisfy:

$$\frac{\partial\phi_3}{\partial \boldsymbol{n}_3}=-\varepsilon\frac{\partial\phi_2}{\partial \boldsymbol{n}_2}\,,\ \text{on CDEF,} \tag{A.11}$$

$$\phi_3=\left(s+\mathrm{i}\,f\right)\phi_2\,,\ \text{on CDEF.} \tag{A.12}$$

On the water bottom, the free surface and the partially reflecting sidewall, the velocity potentials satisfy:

$$\frac{\partial\phi_2}{\partial z}=0\,,\ \text{on CF,} \tag{A.13}$$

$$\frac{\partial\phi_3}{\partial z}=0\,,\ \text{on BC or FG,} \tag{A.14}$$

$$\frac{\partial \phi_3}{\partial z} = \frac{\omega^2}{g}\phi_3 \text{ , on HA,} \tag{A.15}$$

$$\frac{\partial \phi_3}{\partial x} = \mu k_{0x}\phi_3 \text{ , on GH.} \tag{A.16}$$

We substitute Eqs. (A.10)-(A.16) into Eq. (A.3) and solve Eq. (A.3) to determine the velocity potentials and their normal derivatives on all boundary elements. Then, the reflection coefficient is estimated using Eqs. (A.9) and (26).

REFERENCES

Ang, W. T. (2007). A Beginner's Course in Boundary Element Methods. Universal Publishers, Boca Raton, USA.

Chang, H. K. and J. C. Liou (2006). Solving wave dispersion equation for dissipative media using homotopy perturbation technique. Journal of Waterway, Port, Coastal, and Ocean Engineering 132(1), 28-35.

Chen, H. B., C. P. Tsai and J. R. Chiu (2006). Wave reflection from vertical breakwater with porous structure. Ocean Engineering 33(13), 1705-1717.

Cheng, Y. Z., C. B. Jiang and Y. X. Wang (2009). A coupled numerical model of wave interaction with porous medium. Ocean Engineering 36(12), 952-959.

Dalrymple, R. A., M. A. Losada and P. A. Martin (1991). Reflection and transmission from porous structures under oblique wave attack. Journal of Fluid Mechanics 224, 625-644.

Elchahal, G., R. Younes and P. Lafon (2008). The effects of reflection coefficient of the harbor sidewall on the performance of floating breakwaters. Ocean Engineering 35(11), 1102-1112.

Goda, Y. (2010). Random Seas and Design of Maritime Structures. World Scientific, Singapore.

Ijima, T., C. R. Chou and A. Yoshida (1976). Method of analyses for two-dimensional water wave problems. Proceedings of the 15th Coastal Engineering Conference, Honolulu, Hawaii, 2717-2736.

Isaacson, M. and S. Qu (1990). Waves in a harbour with partially reflecting boundaries. Coastal Engineering 14(3), 193-214.

Jeng, D. S., C. Schacht and C. Lemckert (2005). Experimental study on ocean waves propagating over a submerged breakwater in front of a vertical seawall. Ocean Engineering 32(17), 2231-2240.

Ko, C. H., C. P. Tsai, Y. C. Chen and T. O. Sihombing (2015). Numerical simulations of wave and flow variations between submerged breakwaters and slope seawall. The Twenty-fifth International Offshore and Polar Engineering Conference, Hawaii, USA, 1448-1453.

Koley, S., H. Behera and T. Sahoo (2015). Oblique wave trapping by porous structures near a wall. Journal of Engineering Mechanics 141(3), 04014122.

Koraim, A. S., E. M. Heikal and A. A. Zaid (2014). Hydrodynamic characteristics of porous seawall protected by submerged breakwater. Applied Ocean Research 46, 1-14.

Lan, Y. J., T. W. Hsu, J. W. Lai, C. C. Chwang and C. H. Ting (2011). Bragg scattering of waves propagating over a series of poro-elastic submerged breakwaters. Wave Motion 48(1), 1-12.

Lara, J. L., N. Garcia and I. J. Losada (2006). RANS modelling applied to random wave interaction with submerged permeable structures. Coastal Engineering 53(5), 395-417.

Lee, J. F., L. F. Tu and C. C. Liu (2014). Nonlinear wave evolution above rectangular submerged structures. Journal of Marine Science and Technology 22(5), 531-541.

Liao, S. H., Z. Y. Ji and W. D. Zhu (2006). Research and engineering practice on submerged breakwaters for promoting siltation in Shengli oil field. Proceedings of the Academic Annual Conference, Chinese Hydraulic Engineering Society, Hefei, 240-244.

Liao, Y. C., J. H. Jiang, Y. P. Wu and C. P. Lee (2013). Experimental study of wave breaking criteria and energy loss caused by a submerged porous breakwater on horizontal bottom. Journal of Marine Science and Technology 21(1), 35-41.

Liu, Y., H. J. Li and Y. C. Li (2012). A new analytical solution for wave scattering by a submerged horizontal porous plate with finite thickness. Ocean Engineering 42, 83-92.

Losada, I. J., R. Silva and M. A. Losada (1996). 3-D non-breaking regular wave interaction with submerged breakwaters. Coastal Engineering 28(1), 229-248.

Mendez, F. J. and I. J. Losada (2004). A perturbation method to solve dispersion equations for water waves over dissipative media. Coastal Engineering 51(1), 81-89.

Muni-Reddy, M. G. and S. Neelamani (2006). Wave interaction with caisson defenced by an offshore low-crested breakwater. Journal of Coastal Research SI 39, 1767-1770.

Neves, M. D. G., I. J. Losada and M. A. Losada (2000). Short-wave and wave group scattering by submerged porous plate. Journal of Engineering Mechanics 126(10), 1048-1056.

Sollitt, C. K. and R. H. Cross (1972). Wave transmission through permeable breakwaters. Proceedings of the 13th Coastal Engineering Conference, Vancouver, 1827-1846.

Sulisz, W. (1985). Wave reflection and transmission at permeable breakwater of arbitrary cross-section. Coastal Engineering 9(4), 371-386.

Tsai, C. P., C. H. Yu, H. B. Chen and H. Y. Chen (2012). Wave height transformation and set-up between a submerged permeable breakwater and a seawall. China Ocean Engineering 26, 167-176.

Twu, S. W. and C. C. Liu (2004). Interaction of non-breaking regular waves with a periodic array of artificial porous bars. Coastal engineering 51(3), 223-236.

Wu, Y. T., C. L. Yeh and S. C. Hsiao (2014). Three-dimensional numerical simulation on the interaction of solitary waves and porous breakwaters. Coastal Engineering 85, 12-29.

Yu, X. P. (1995). Diffraction of water waves by porous breakwaters. Journal of Waterway, Port, Coastal, and Ocean Engineering 121(6), 275-282.

Yu, X. P. and A. T. Chwang (1994). Wave motion through porous structures. Journal of Engineering Mechanics 120(5), 989-1008.

Yueh, C. Y. and S. H. Chuang (2009). The reflection of normal incident waves by absorbing-type breakwaters. China Ocean Engineering 23(4), 729-740.

Zhang, J. S., D. S. Jeng, P. L. F. Liu, C. Zhang and Y. Zhang (2012). Response of a porous seabed to water waves over permeable submerged breakwaters with Bragg reflection. Ocean Engineering 43, 1-12.